

Channel Attention with Embedding Gaussian Process: A Probabilistic Methodology*

Jiyang Xie¹, Dongliang Chang¹, Zhanyu Ma^{1†}, Guoqiang Zhang² and Jun Guo¹

¹Pattern Recognition and Intelligent Systems Lab., Beijing University of Posts and Telecommunications, Beijing, China

²School of Electrical and Data Engineering, University of Technology Sydney, Sydney, Australia
{xiejiyang2013, changdongliang, mazhanyu, guojun}@bupt.edu.cn, guoqiang.zhang@uts.edu.au

Abstract

Channel attention mechanisms, as the key components of some modern convolutional neural networks (CNNs) architectures, have been commonly used in many visual tasks for effective performance improvement. It is able to reinforce the informative channels and to suppress useless channels of feature maps obtained by CNNs. Recently, different attention modules have been proposed, which are implemented in various ways. However, they are mainly based on convolution and pooling operations, which are lack of intuitive and reasonable insights about the principles that they are based on. Moreover, the ways that they improve the performance of the CNNs is not clear either. In this paper, we propose a Gaussian process embedded channel attention (GPCA) module and interpret the channel attention intuitively and reasonably in a probabilistic way. The GPCA module is able to model the correlations from channels which are assumed as beta distributed variables with Gaussian process prior. As the beta distribution is intractably integrated into the end-to-end training of the CNNs, we utilize an appropriate approximation of the beta distribution to make the distribution assumption implemented easily. In this case, the proposed GPCA module can be integrated into the end-to-end training of the CNNs. Experimental results demonstrate that the proposed GPCA module can improve the accuracies of image classification on four widely used datasets.

1 Introduction

Deep neural networks have attracted great attention and pushed the performance of various computer vision and image processing tasks from academic to industry including image classification [Simonyan and Zisserman, 2015; He *et al.*, 2016; Huang *et al.*, 2017], image retrieval [Ma *et al.*, 2019; Xu *et al.*, 2018a; Xu *et al.*, 2018b], object detection [Liu *et al.*, 2016; Ren *et al.*, 2015], and semantic segmentation

[Badrinarayanan *et al.*, 2017; Chen *et al.*, 2018]. Convolutional neural networks (CNNs) as well-known deep neural network architectures are able to effectively capture the discriminative nonlinear patterns from images, extract feature representations, and generate multi-channel feature maps. This phenomena are mainly due to their deep and wide structures and introduction of additional network components including dropout [Hinton *et al.*, 2012] and attention [Vaswani *et al.*, 2017].

Attention mechanisms as the key components of modern CNN architectures are generally located behind some specific convolutional layers, such as the last layers in each residual block of ResNet [He *et al.*, 2016]. They have been utilized for feature recalibration with attention weights and widely applied to effectively improve the performance of the CNNs learned from large-scale datasets [Hu *et al.*, 2018b]. Previous literatures [Jaderberg *et al.*, 2015; Woo *et al.*, 2018; Hu *et al.*, 2018b] have studied the significance of the attention mechanisms. Attention can not only inform the CNNs about their concentrations on a image or features extracted by them, but also develop the feature representation of the image [Woo *et al.*, 2018].

Channel attention, which is a significant part of the attention mechanisms, aims to improve the quality of feature representations by precisely modelling the correlations between the channels of the convolutional feature maps [Hu *et al.*, 2018b]. It is able to enhance the informative and discriminative feature maps and suppress the useless and unhelpful ones simultaneously by learning the attention weights for each channel which are optimized in an implicit way.

Relevant works [Hu *et al.*, 2018b; Hu *et al.*, 2018a; Woo *et al.*, 2018; Sun *et al.*, 2018; Park *et al.*, 2018; Huang *et al.*, 2019; Yang *et al.*, 2019; Luo *et al.*, 2019; Lopez *et al.*, 2019] have proposed different attention modules in different implementation ways. However, all these works are based on the convolutional operations and pooling which are lack of intuitive and reasonable explanations about why they work well and how they can improve the performance of CNNs remarkably.

In this paper, we propose an attention mechanism, so-called *Gaussian process embedded channel attention (GPCA)*, to clarify the channel attention mechanism intuitively and reasonably in a probabilistic way. We assume the channel attention masks are drawn from or follow inde-

*Under review.

†Corresponding Author.

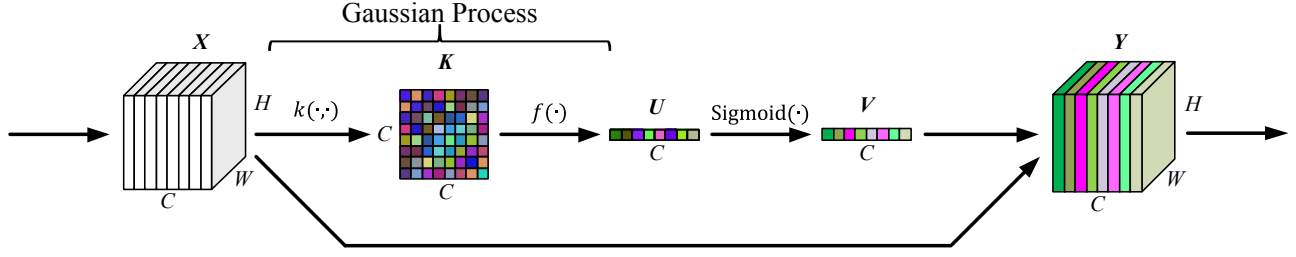


Figure 1: Structure of the Gaussian process embedded channel attention (GPCA) module.

pendent beta distributions with $[0, 1]$ bound, which is a common boundary condition of traditional attentions. Given that a channel attention module learns the weights of channels by computing their correlations precisely within end-to-end training, Gaussian process [Bishop, 2006], which is a popular Bayesian learning framework and usually used for extracting relationship between one sample and others, is integrated into the GPCA module as the prior of the beta distributed variables. This is for the purpose of learning the correlations among different channels in an explicit way. In this case, the informative channels can be emphasised by large values of attention masks, extracted by the GPCA module based on the channels. Experimental results show that the proposed GPCA module can considerably improve the accuracies on four image classification datasets.

2 Related Work

Attention mechanisms are well-known and play important roles in image classification task [Hu *et al.*, 2018b; Hu *et al.*, 2018a; Woo *et al.*, 2018; Park *et al.*, 2018; Luo *et al.*, 2019; Lopez *et al.*, 2019; Li *et al.*, 2019]. Most of the aforementioned works discuss what is the most effective way for introducing the attention mechanisms in their models. These works concentrate on driving CNNs to focus on informative channels and/or regions of convolutional feature maps.

To this end, squeeze-and-excitation network (SENet) [Hu *et al.*, 2018b], which has been widely used in various network architectures, was proposed to investigate the channel relationship by squeezing and exciting the channels, and yielded significant improvements of performance. In addition, gather-excite network (GENet) [Hu *et al.*, 2018a] introduced a parametric gather-excite operator pair into the residual blocks in ResNet [He *et al.*, 2016], which aggregated the feature responses across the spatial neighbourhoods in a feature map and redistributed the local features via nearest neighbour interpolation. In addition, stochastic region pooling (SRP) [Luo *et al.*, 2019], a channel attention module, randomly selected square regions from feature maps to extract the channel descriptors and forcing them to be more representative and less homogeneous. Then, it excited the channel descriptors in a similar way as the SENet to produce the channel attention masks.

Spatial attention is commonly combined with the channel attention in CNNs to further regularize the feature maps. Bottleneck attention module (BAM) [Park *et al.*, 2018] created two separate and parallel pathways, *i.e.*, the channel-wise

and the spatial-wise ones, to construct channel and spatial attentions. It combined them together as an element-wise attention. Meanwhile, different from the BAM, convolutional block attention module (CBAM) [Woo *et al.*, 2018] inferred the element-wise attention maps by the cascade-connected channel and spatial attentions for adaptive refinement of the intermediate feature maps.

There are still other attention-related works which integrate channel attention mechanisms for special motivations. The work in [Lopez *et al.*, 2019] captured the channel attentions after each convolutional block for rectifying the output likelihood distributions of the whole CNN, rather than the corresponding feature maps in the blocks. This can be considered as an output attention (OA) mechanism. In addition, the channel attention mechanism has been utilized for convolutional kernel selection. Selective kernel network (SKNet) [Li *et al.*, 2019] was proposed to dynamically adjust the receptive field sizes of convolutional layers in CNNs by weighting the parallel convolutional kernels with different kernel sizes in a convolutional layer.

3 Gaussian Process Embedded Channel Attention (GPCA)

A Gaussian process embedded channel attention (GPCA) module can learn the correlations between channels in CNNs via a Gaussian process [Bishop, 2006] and calibrate the input feature maps by multiple channel-wise masks. We define the input feature maps by $\mathbf{X} \in R^{C \times W \times H}$ as shown in Figure 1, where C , W , and H are the channel number, the width and the height of feature maps, respectively. Meanwhile, the final output $\mathbf{Y} \in R^{C \times W \times H}$ of the GPCA module is obtained by scaling \mathbf{X} with the attention mask vector $\mathbf{V} = [v_1, \dots, v_C]^T$ as

$$\mathbf{Y}_c = v_c \cdot \mathbf{X}_c, \quad (1)$$

where \mathbf{Y}_c and \mathbf{X}_c are the c^{th} channel of \mathbf{Y} and \mathbf{X} , respectively, and $c = 1, \dots, C$.

Here, the element v_c of the attention mask vector \mathbf{V} is commonly set as a $[0, 1]$ -bounded variable [Hu *et al.*, 2018b; Hu *et al.*, 2018a; Woo *et al.*, 2018; Park *et al.*, 2018] to scale the input feature maps with the normalized importance weights. Thus, we assume that the elements in \mathbf{V} follow independent beta distributions to represent the importance of the channels. The probability density function (PDF) of the

beta distribution is defined as

$$\text{Beta}(x; \alpha, \beta) = \frac{x^{\alpha-1}(1-x)^{\beta-1}}{\text{B}(\alpha, \beta)}, \quad (2)$$

where $\text{B}(\alpha, \beta) = \frac{\Gamma(\alpha)\Gamma(\beta)}{\Gamma(\alpha+\beta)}$ and $\Gamma(\cdot)$ is the Gamma function. The beta distribution, as a member of the exponential family, is defined in a bounded interval, *i.e.*, $[0, 1]$, which is consistent with the definition of the channel attention. Meanwhile, the beta distribution is used for describing the statistical behavior of percentages and proportions in Bayesian learning like certainty or importance. This further satisfies the principles of the attention modelling. In addition, it has flexible shapes (*i.e.*, bell, U, and uniform shapes) depending on the values of the parameters α and β , which makes it suitable for the channel attention learning in general.

However, although the beta PDF is differentiable in the interval of $(0, 1)$, the beta distribution is unfeasible to be directly extended in the CNN training, as discussed in [Xie *et al.*, 2019]. Thus, we introduce an approximated beta distribution $q(\alpha, \beta)$, named the Sigmoid-Gaussian assumption. A random variable $v \sim q(\alpha, \beta)$ following the distribution assumption can be generated by transferring a Gaussian distributed variable $u \sim \mathcal{N}(\mu, \sigma^2)$ as

$$v = \text{Sigmoid}(u) = \frac{1}{1 + e^{-u}}, \quad (3)$$

and parameters α and β can be estimated by solving equations of moment matching as

$$\begin{cases} \mu = \phi(\alpha) - \phi(\beta) \\ \sigma^2 = \phi_1(\alpha) + \phi_1(\beta) \end{cases}, \quad (4)$$

where $\phi(\cdot)$ and $\phi_1(\cdot)$ are the digamma and trigamma functions, respectively.¹ As it can be easily proven that the integration $\int_0^1 q(v; \alpha, \beta) dv$ is equal to 1, the elements $v_c \sim q(\alpha_c, \beta_c) = q(\mu_c, \sigma_c)$, $c = 1, \dots, C$ of \mathbf{V} are the random variables which all follow normalized distributions, respectively. To demonstrate the effectiveness of the Sigmoid-Gaussian assumption, we conduct several groups of experiments with different parameters of Gaussian distribution and calculate the Kullback-Leibler (KL) divergences from the PDFs q of the Sigmoid-Gaussian assumption to the estimated beta PDFs p with parameters α and β from q in each group, as shown in Figure 2. It can be observed that the q yield reasonable and accurate approximation to the corresponding p with small KL divergences, which can clearly show that the effectiveness of this approximation.

Then, we introduce a Gaussian process prior $\mathcal{GP}(\cdot)$ with input \mathbf{X} for \mathbf{U} as $\mathbf{U} \sim \mathcal{GP}(\mathbf{X})$. Here we consider the channels in \mathbf{X} as the samples in $\mathcal{GP}(\cdot)$. Although we cannot obtain any exact targets of attention masks in CNNs, we are able to learn the channel correlations in \mathbf{X} by \mathbf{a}^* and $\mathbf{a}_c^* \in R^{1 \times C^*}$ ($C^* = C - 1$) for the c^{th} channel to others, which is defined as

$$\mathbf{a}_c^* = \mathbf{K}_{\mathbf{x}_c, \mathbf{x}_{i \neq c}} (\mathbf{K}_{\mathbf{x}_{i \neq c}, \mathbf{x}_{i \neq c}} + \delta^{-1} \mathbf{I}_{C^*})^{-1}, \quad (5)$$

¹Please refer to https://en.wikipedia.org/wiki/Beta_distribution.

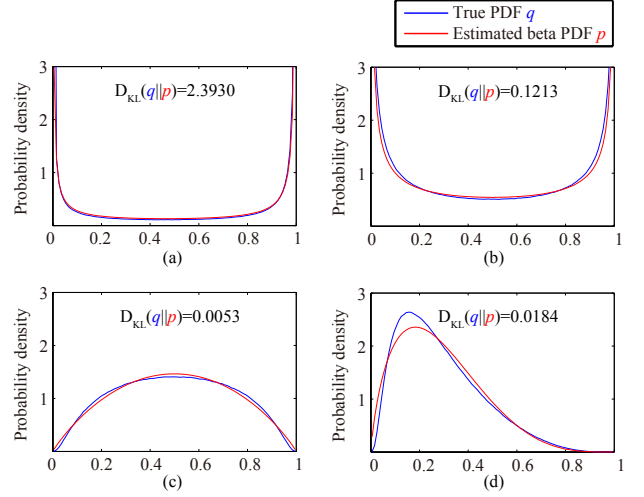


Figure 2: Comparison of the true probability density function (PDF) q generated by the Sigmoid-Gaussian assumption and the estimated beta PDF p from q . D_{KL} denotes Kullback-Leibler (KL) divergence. (a) q with parameters $\mu = 8.5$ and $\sigma = 10$ and p with parameters $\alpha = 0.18$ and $\beta = 0.05$; (b) q with $\mu = 0$ and $\sigma = 3$ and p with $\alpha = 0.4$ and $\beta = 0.4$; (c) q with $\mu = 0$ and $\sigma = 1$ and p with $\alpha = 1.91$ and $\beta = 1.91$; (d) q with $\mu = -1$ and $\sigma = 1$ and p with $\alpha = 1.77$ and $\beta = 4.46$.

where \mathbf{x}_c represents the c^{th} channel of \mathbf{X} , $\mathbf{x}_{i \neq c}$ represents the other channels of \mathbf{X} except \mathbf{x}_c , δ represents the precision of the Gaussian assumption in the Gaussian process which is set as one in practice, and \mathbf{I}_{C^*} is an $C^* \times C^*$ identity matrix. \mathbf{K} is the Gram matrix in the Gaussian process [Bishop, 2006] with elements $K_{c,c'}, c, c' = 1, \dots, C$, as

$$K_{c,c'} = k(\mathbf{x}_c, \mathbf{x}_{c'}) = \underbrace{\theta_0 e^{-\theta_1 \|\mathbf{x}_c - \mathbf{x}_{c'}\|^2}}_{\text{Gaussian kernel}} + \underbrace{\theta_2}_{\text{Bias}} + \underbrace{\theta_3 \mathbf{x}_c \mathbf{x}_{c'}^T}_{\text{Linear kernel}}, \quad (6)$$

where $k(\mathbf{x}_c, \mathbf{x}_{c'})$ is a kernel function with nonnegative hyperparameters $\Theta = \{\theta_0, \theta_1, \theta_2, \theta_3\}$ and consists of a Gaussian kernel, a linear kernel, and a bias. $\mathbf{K}_{\mathbf{x}_c, \mathbf{x}_{i \neq c}}$ and $\mathbf{K}_{\mathbf{x}_{i \neq c}, \mathbf{x}_{i \neq c}}$ are parts of \mathbf{K} . Due to the correlation calculated between a vector itself equal to 1, we modify \mathbf{a}_c^* to $\mathbf{a}_c \in R^C$, $c = 1, \dots, C$ as

$$\mathbf{a}_{c,i} = \begin{cases} \mathbf{a}_{c,i}^*, & i < c \\ 1, & i = c \\ \mathbf{a}_{c,i-1}^*, & i > c \end{cases}. \quad (7)$$

Then, we assume the importance weight vector $\mathbf{U} \in R^C$ for each channel in Figure 1 following independently Gaussian distributions as

$$\mathbf{U} \sim \prod_c \mathcal{N}(A_c, B_c), \quad (8)$$

where A_c, B_c are the mean and the variance of u_c , respectively. They can be calculated as

Table 1: Statistics of all four datasets including class number, training and test sample number in each class, and the input image size.

Dataset	#class	#training	#test	Image size
Cifar-10	10	5000	1000	32×32
Cifar-100	100	500	100	32×32
<i>mini</i> ImageNet	100	500	100	224×224
ImageNet 32×32	1000	1300	50	32×32

$$A_c = \frac{1}{C} \sum_{c'=1}^C a_{c',c}, \quad (9)$$

$$B_c = K_{x_c, x_c} - a_c K_{x_c, x_{i \neq c}}^T. \quad (10)$$

Here, we define the mapping $f(\cdot)$ in Figure 1 for learning U from K as $U = f(K)$. In practice, the expectation of the random variable v_c is considered as the final GPCA mask of the c^{th} channel, which can be calculated by [Bishop, 2006]

$$E[v_c] \approx \text{Sigmoid} \left(\frac{A_c}{\sqrt{1 + \frac{\pi}{8} B_c}} \right). \quad (11)$$

4 Experimental Results and Discussions

In this section, we evaluate the performance of the proposed GPCA module by comparisons with five attention modules, *i.e.*, SENet [Hu *et al.*, 2018b], BAM [Park *et al.*, 2018], CBAM [Woo *et al.*, 2018], SRP [Luo *et al.*, 2019], OA [Lopez *et al.*, 2019], on four datasets in the image classification task.

4.1 Datasets

We evaluate the proposed GPCA module on four image classification datasets, including Cifar-10/-100 [Krizhevsky, 2009] datasets, *mini*ImageNet [Vinyals *et al.*, 2016], and ImageNet- 32×32 [Den Oord *et al.*, 2016] datasets, respectively. The detailed summary of the datasets is listed in Table 1. In the *mini*ImageNet dataset, 500 and 100 images of per class are respectively randomly selected from the full ImageNet dataset as training and test sets. The ImageNet- 32×32 dataset is more difficult than the full ImageNet dataset and all the images are resized to 32×32 for training and test.

4.2 Implementation Details

For the Cifar-10 and the Cifar-100 datasets, VGG16 [Simonyan and Zisserman, 2015] and ResNet50 [He *et al.*, 2016] models were used as the base models for the proposed GPCA and other referred modules. Adopting the stochastic gradient descent (SGD) optimizer, we trained each model 300 epochs with batch size of 256, and the initial learning rates were set as 0.1 and decayed by a factor of 10 at the 150^{th} and the 225^{th} epochs. The momentum and the weight decay values were kept as 0.9 and 5×10^{-4} , respectively. All the methods were conducted three times with random initialization and the means of the classification accuracies are reported.

For the *mini*ImageNet and the ImageNet- 32×32 datasets, the VGG16, the ResNet18, and the ResNet34 models were

Table 2: Test accuracies (%) on the Cifar-10 and the Cifar-100 datasets. Note that the best and the second best results of each base model are marked in **bold** and *italic* fonts, respectively.

Model	Cifar-10	Cifar-100
VGG16 (baseline)	93.90	73.64
VGG16+SE (2018)	94.04	73.86
VGG16+CBAM-S (2018)	94.12	74.31
VGG16+GPCA-fixed (ours)	<i>94.50</i>	<i>74.59</i>
VGG16+GPCA (ours)	94.51	74.65
ResNet50 (baseline)	93.52	71.88
ResNet50+SE (2018)	94.16	72.64
ResNet50+BAM (2018)	94.14	73.36
ResNet50+CBAM (2018)	94.06	73.01
ResNet50+CBAM-S (2018)	94.00	73.29
ResNet50+SRP (2019)	94.11	72.25
ResNet50+OA (2019)	94.09	72.73
ResNet50+GPCA-fixed (ours)	<i>94.87</i>	<i>73.84</i>
ResNet50+GPCA (ours)	94.93	73.93

used as the base models for all the methods, and the settings of the optimizers and the initial learning rates were same with the other two datasets. We trained each model 300 and 100 epochs with batch sizes of 128 and 256 on the two datasets, respectively. Meanwhile, the learning rate on the *mini*ImageNet dataset was decayed by a factor of 10 at the 150^{th} and the 225^{th} epochs, which were the 50^{th} and the 75^{th} epochs on the other dataset.

The parameters Θ are optimized during training. To investigate the effectiveness of the optimization, the classification accuracies of the fixed-parameter version (model_name+GPCA-fixed) are also reported as ablation study, in which the optimal parameter Θ are manually selected.

All the attention modules were added in each residual block in the ResNets, but they were only applied after the last convolutional layer of the VGG16 model. Note that in a VGG16 model, the output size of feature maps of the last convolutional layer was $512 \times 1 \times 1$ while the size of input images was $3 \times 32 \times 32$ (*i.e.*, the Cifar-10, the Cifar-100, and the ImageNet- 32×32 datasets), and the BAM, the CBAM, and the SRP cannot work in this case. However, the channel attention of the CBAM can be separately applied in a VGG16 model, named CBAM-S. In addition, the OA needed to be used in multiple blocks and cannot be implemented in the VGG16 model either on all the datasets.

4.3 Performance on Cifar-10/-100 Datasets

From Table 2, the proposed GPCA module performs the best among the other methods with both VGG16 and ResNet50 models on both Cifar-10 and Cifar-100 datasets. Firstly, on the Cifar-10 dataset, the proposed GPCA module achieves the classification accuracies at 94.51% and 94.93% based on the VGG16 and the ResNet50 models, respectively, and outperforms the fixed-parameter version slightly. Meanwhile, the proposed GPCA module with the VGG16 and the ResNet50 models exceed their own base models, *i.e.*, the VGG-16 and

Table 3: Test accuracies (acc., %) on the *mini*ImageNet dataset. Note that the best and the second best results of each base model are marked in **bold** and *italic* fonts, respectively.

Model	Acc.
VGG16 (baseline)	81.36
VGG16+SE (2018)	81.66
VGG16+BAM (2018)	81.38
VGG16+CBAM (2018)	81.42
VGG16+CBAM-S (2018)	81.62
VGG16+SRP (2019)	81.91
VGG16+GPCA-fixed (ours)	<i>82.52</i>
VGG16+GPCA (ours)	82.78
ResNet18 (baseline)	77.13
ResNet18+SE (2018)	77.76
ResNet18+BAM (2018)	77.87
ResNet18+CBAM (2018)	77.62
ResNet18+CBAM-S (2018)	78.02
ResNet18+SRP (2019)	77.93
ResNet18+OA (2019)	77.49
ResNet18+GPCA-fixed (ours)	<i>78.85</i>
ResNet18+GPCA (ours)	78.87
ResNet34 (baseline)	78.08
ResNet34+SE (2018)	78.44
ResNet34+BAM (2018)	78.23
ResNet34+CBAM (2018)	78.16
ResNet34+CBAM-S (2018)	78.46
ResNet34+SRP (2019)	78.99
ResNet34+OA (2019)	78.14
ResNet34+GPCA-fixed (ours)	<i>79.92</i>
ResNet34+GPCA (ours)	80.14

the ResNet50 models, at about 0.6% and 1.4%, respectively. Moreover, the proposed GPCA module with the VGG16 model outperforms the CBAM-S module (94.12%), the best referred method, at about 0.4%, while the proposed GPCA module with the ResNet50 model surpasses the SE module with the ResNet50 model (94.16%) more than 0.8%.

Similarly on the Cifar-100 dataset, the proposed GPCA module achieves the classification accuracies at 74.65% and 73.93% on the VGG16 and the ResNet50 base models, respectively, with the fixed-parameter version at 74.59% and 73.84%. It performs best among the referred methods as shown in Table 2. The GPCA-based VGG16 and ResNet50 models have moderate improvements compared with the corresponding base models at more than 1% and 2%, respectively. In addition, they also gain about 0.3% and 0.6% improvements compared with the best referred models, *i.e.*, the CBAM-S module with the VGG16 (74.31%) and the BAM module with the ResNet50 (73.36%) models, respectively.

4.4 Performance on *Mini*ImageNet Dataset

In Table 3, the proposed GPCA module obtained the best results with VGG16, ResNet18 and ResNet34 models among the referred methods on the *mini*ImageNet dataset, which achieves the classification accuracies at 82.78%, 78.87%, and 80.14%, respectively. Applying the VGG16 model as the

Table 4: Top-1 and top-5 test accuracies (acc., %) on the ImageNet-32×32 dataset. Note that the best and the second best results of each base model are marked in **bold** and *italic* fonts, respectively.

Model	Top-1 acc.	Top-5 acc.
VGG16 (baseline)	39.70	62.66
VGG16+SE (2018)	39.82	62.99
VGG16+CBAM-S (2018)	39.56	62.84
VGG16+GPCA-fixed (ours)	<i>42.15</i>	<i>65.35</i>
VGG16+GPCA (ours)	42.58	65.65
ResNet18 (baseline)	47.75	72.70
ResNet18+SE (2018)	47.89	72.98
ResNet18+BAM (2018)	47.90	73.08
ResNet18+CBAM (2018)	48.48	73.25
ResNet18+CBAM-S (2018)	48.31	73.37
ResNet18+SRP (2019)	48.84	73.74
ResNet18+OA (2019)	48.62	73.21
ResNet18+GPCA-fixed (ours)	<i>49.34</i>	<i>74.88</i>
ResNet18+GPCA (ours)	49.58	75.07
ResNet34 (baseline)	49.82	74.34
ResNet34+SE (2018)	50.30	74.89
ResNet34+BAM (2018)	<i>50.70</i>	74.79
ResNet34+CBAM (2018)	<i>50.28</i>	74.89
ResNet34+CBAM-S (2018)	50.65	75.07
ResNet34+SRP (2019)	50.24	74.73
ResNet34+OA (2019)	50.04	74.88
ResNet34+GPCA-fixed (ours)	50.65	<i>75.46</i>
ResNet34+GPCA (ours)	51.24	75.79

base model, the classification accuracy of the GPCA with the VGG16 model is larger than 82.5%; however, the accuracies obtained by the other referred models are all smaller than 82%. It outperforms the base model at about 1.4% and the best referred method, the SRP with the VGG16 model, at more than 0.8%. Furthermore, the ResNet-based GPCA models also have improvement on classification accuracies on the *mini*ImageNet dataset. Compared with their base models, the GPCA with the ResNet18 and the ResNet34 models increase their accuracies about 1.7% and 2.1%, respectively, which are considerable performance improvements. Meanwhile, they respectively surpass the CBAM-S with the ResNet18 (78.02%) and the SRP with the ResNet34 (78.99%) models more than 0.8% and 1.1%, respectively.

4.5 Performance on ImageNet-32 × 32 Dataset

In Table 4, the proposed GPCA modules with the VGG16, the ResNet18, and the ResNet34 models perform the best on the ImageNet-32 × 32 dataset and respectively achieve the top-1 accuracies of 42.58%, 49.58%, and 51.24%, and the top-5 accuracies of 65.65%, 75.07%, and 75.79%. Compared with their corresponding base models, the models based on the proposed GPCA module improve the accuracies by a large margin. Applying the VGG16 model as the base model, the classification accuracy of the GPCA-based model outperforms the second best model, the SE module with the VGG16 model, at 2.8% on top-1 and 2.7% on top-5, which are marked performance improvements. Meanwhile, with the ResNet18

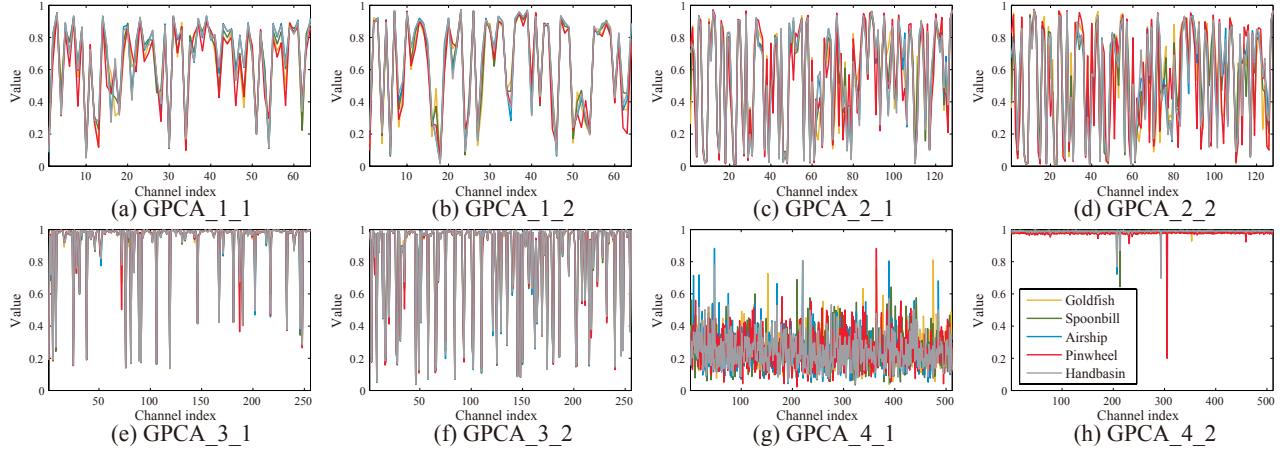


Figure 3: Values of the attention masks at different depths in the GPCA module with the ResNet18 on the ImageNet- 32×32 dataset. The modules in each subfigure is named as GPCA_stageID.blockID. The stageID and blockID are in the sets of $\{1, 2, 3, 4\}$ and $\{1, 2\}$ for a ResNet18. **Note that all the subfigures share the same captions as shown in (h).**

base model, the GPCA-based model has considerable performance improvements compared with the base model and the second best model as well. Compared with the base model, the proposed GPCA with the ResNet18 model achieves 1.8% and 2.4% improvements on top-1 and top-5 accuracies, respectively. Moreover, it improves the accuracies at 0.7% on top-1 and 1.3% on top-5 than the best referred model, the SRP module with the ResNet18 model. Meanwhile, with the ResNet34 model, the proposed GPCA module achieves the best accuracies on both top-1 and top-5, although the fixed-parameter version obtains a slight drop compared with the best referred method on top-1 accuracy.

4.6 Role of the GPCA Module

To investigate the role of the GPCA module in CNNs, we illustrate the distribution of the values of the attention masks learned by the GPCA module for different classes. We selected five classes, termed goldfish, spoonbill, airship, pinwheel, and washbasin, from the ImageNet- 32×32 dataset and drew the averaged values of the attention masks on each channel of all the test samples in the corresponding classes, as shown in Figure 3. The ResNet18 model was used as the base model. It can be observed that the GPCA masks for different classes are distinct in most of the channels at the shallower blocks such as GPCA_1_1 and GPCA_2_2, which means that different channels focus on different texture patterns. Meanwhile, we observe that different channels have diverse importance weights at the shallower stages (stage 1 and 2). This indicates that some channels with smaller attention values are less significant for classification and can be pruned, for example, channel 10 in GPCA_1_1.

In addition, for the deeper blocks in a ResNet18 model such as GPCA_3_1, GPCA_3_2 and GPCA_4_2, the GPCA masks converge towards the same values. An interesting tendency can be found that some deeper blocks such as GPCA_3_1, GPCA_3_2 and GPCA_4_2 tend to learn the attention masks close to one on most of the channels with the outliers approaching zero. This suggests that most of the chan-

nels provide semantic information with same significance in the classes for classification and different classes require to be classified by using all the information.

Thus, The effectiveness of the GPCA module can be clarified since the GPCA modules perform as channel-wise feature selectors and play distinct and important roles in different depths of the ResNet18 model. In addition, similar phenomena can be also observed on the other datasets, and in the VGG16 and the ResNet34 models, respectively.

4.7 Discussions

In this section, we will discuss how the GPCA module works. To model the attention masks of the GPCA module, we assume them following independent beta distributions with $[0, 1]$ bound, which is a common boundary condition of traditional attentions. Training a channel attention module for the outputs of a specific convolutional layer can be defined as a regression task *implicitly* targeted the outputs of the whole CNN model, given that the correlations of channels are learned by the network itself according to the gradients of backpropagation without any explicit targets of the correlations. Gaussian process [Bishop, 2006] is competent to do this job due to its capability of correlation computation between samples. In this case, we introduce the Gaussian process prior to the beta assumption for extracting the relationship between the channels of convolutional layers based on the global channel information from the feature maps *in an explicit way* and obtain the importance weights of each channel to emphasise the informative channels.

5 Conclusions

In this paper, we proposed a Gaussian process embedded channel attention (GPCA) module to learn the correlations from the channels in CNNs. In the proposed GPCA module, the output channel attention masks are assumed as beta distributed variables with a Gaussian process prior. In this case, the proposed GPCA module can be intuitively and reasonably clarified in a probabilistic way. Although the beta dis-

tribution has difficulty to be integrated into end-to-end training of the CNNs, we utilized an appropriate approximation of the beta distribution. Furthermore, experimental results show that the proposed GPCA module can be end-to-end trained on the widely used base models and considerably improve the accuracies on four benchmark image classification datasets, compared with five referred attention modules.

References

- [Badrinarayanan *et al.*, 2017] V. Badrinarayanan, A. Kendall, and R. Cipolla. SegNet: A deep convolutional encoder-decoder architecture for image segmentation. *IEEE Transactions on Pattern Analysis and Machine Intelligence*, 39(12):2481–2495, 2017.
- [Bishop, 2006] C. M. Bishop. *Pattern Recognition and Machine Learning*. Springer Science+Business Media LLC., 2006.
- [Chen *et al.*, 2018] L. Chen, G. Papandreou, I. Kokkinos, K. Murphy, and A. L. Yuille. DeepLab: Semantic image segmentation with deep convolutional nets, atrous convolution, and fully connected CRFs. *IEEE Transactions on Pattern Analysis and Machine Intelligence*, 40(4):834–848, 2018.
- [Den Oord *et al.*, 2016] A. V. Den Oord, N. Kalchbrenner, and K. Kavukcuoglu. Pixel recurrent neural networks. *arXiv*, 2016.
- [He *et al.*, 2016] K. He, X. Zhang, S. Ren, and J. Sun. Deep residual learning for image recognition. In *Computer Vision and Pattern Recognition*, pages 770–778, 2016.
- [Hinton *et al.*, 2012] G. E. Hinton, N. Srivastava, A. Krizhevsky, I. Sutskever, and R. Salakhutdinov. Improving neural networks by preventing co-adaptation of feature detectors. *arXiv*, 2012.
- [Hu *et al.*, 2018a] J. Hu, L. Shen, S. Albanie, G. Sun, and A. Vedaldi. Gather-excite: Exploiting feature context in convolutional neural networks. In *Neural Information Processing Systems*, pages 9401–9411, 2018.
- [Hu *et al.*, 2018b] J. Hu, L. Q. Shen, and G. Sun. Squeeze-and-excitation networks. In *Computer Vision and Pattern Recognition*, pages 7132–7141, 2018.
- [Huang *et al.*, 2017] G. Huang, Z. Liu, L. V. Der Maaten, and K. Q. Weinberger. Densely connected convolutional networks. In *Computer Vision and Pattern Recognition*, pages 2261–2269, 2017.
- [Huang *et al.*, 2019] Z. Huang, S. Liang, M. Liang, and H. Yang. DIANet: Dense-and-implicit attention network. *arXiv*, 2019.
- [Jaderberg *et al.*, 2015] M. Jaderberg, K. Simonyan, A. Zisserman, and K. Kavukcuoglu. Spatial transformer networks. In *Neural Information Processing Systems*, pages 2017–2025, 2015.
- [Krizhevsky, 2009] A. Krizhevsky. Learning multiple layers of features from tiny images. techreport, CIFAR, 2009.
- [Li *et al.*, 2019] X. Li, W. Wang, X. Hu, and J. Yang. Selective kernel networks. In *Computer Vision and Pattern Recognition*, 2019.
- [Liu *et al.*, 2016] W. Liu, D. Anguelov, D. Erhan, C. Szegedy, S. E. Reed, C. Fu, and A. C. Berg. SSD: Single shot multibox detector. In *European Conference on Computer Vision*, pages 21–37, 2016.
- [Lopez *et al.*, 2019] P. R. Lopez, D. V. Dorta, G. C. Preixens, J. M. G. Sitjes, F. X. R. Marva, and J. Gonzalez. Pay attention to the activations: a modular attention mechanism for fine-grained image recognition. *IEEE Transactions on Multimedia*, 2019.
- [Luo *et al.*, 2019] M. Luo, G. Wen, Y. Hu, D. Dai, and Y. Xu. Stochastic region pooling: Make attention more expressive. *arXiv*, 2019.
- [Ma *et al.*, 2019] Z. Ma, Y. Ding, S. Wen, J. Xie, Y. Jin, Z. Si, and H. Wang. Shoe-print image retrieval with multi-part weighted CNN. *IEEE ACCESS*, 7:59728 – 59736, 2019.
- [Park *et al.*, 2018] J. Park, S. Woo, J. Lee, and I. S. Kweon. BAM: Bottleneck attention module. In *British Machine Vision Conference*, page 147, 2018.
- [Ren *et al.*, 2015] S. Ren, K. He, R. B. Girshick, and J. Sun. Faster R-CNN: Towards real-time object detection with region proposal networks. *arXiv*, 2015.
- [Simonyan and Zisserman, 2015] K. Simonyan and A. Zisserman. Very deep convolutional networks for large-scale image recognition. In *International Conference on Learning Representations*, 2015.
- [Sun *et al.*, 2018] M. Sun, Y. Yuan, F. Zhou, and E. Ding. Multi-attention multi-class constraint for fine-grained image recognition. In *European Conference on Computer Vision*, pages 834–850, 2018.
- [Vaswani *et al.*, 2017] A. Vaswani, N. Shazeer, N. Parmar, J. Uszkoreit, L. Jones, A. N. Gomez, L. Kaiser, and I. Polosukhin. Attention is all you need. In *Neural Information Processing Systems*, pages 5998–6008, 2017.
- [Vinyals *et al.*, 2016] O. Vinyals, C. Blundell, T. P. Lillicrap, K. Kavukcuoglu, and D. Wierstra. Matching networks for one shot learning. *arXiv*, 2016.
- [Woo *et al.*, 2018] S. Woo, J. Park, J. Y. Lee, and I. S. Kweon. CBAM: Convolutional block attention module. In *European Conference on Computer Vision*, pages 3–19, 2018.
- [Xie *et al.*, 2019] J. Xie, Z. Ma, G. Zhang, J.-H. Xue, Z.-H. Tan, and J. Guo. Soft dropout and its variational Bayes approximation. In *IEEE International Workshop on Machine Learning for Signal Processing*, 2019.
- [Xu *et al.*, 2018a] P. Xu, Y. Huang, T. Yuan, K. Pang, Y. Z. Song, T. Xiang, T. M. Hospedales, Z. Ma, and J. Guo. SketchMate: Deep hashing for million-scale human sketch retrieval. In *Computer Vision and Pattern Recognition*, pages 8090–8098, 2018.

- [Xu *et al.*, 2018b] P. Xu, Q. Yin, Y. Huang, Y. Z. Song, Z. Ma, L. Wang, T. Xiang, W. B. Kleijn, and J. Guo. Cross-modal subspace learning for fine-grained sketch-based image retrieval. *Neurocomputing*, 278:75–86, 2018.
- [Yang *et al.*, 2019] Y. Yang, X. Wang, Q. Zhao, and T. Sui. Two-level attentions and grouping attention convolutional network for fine-grained image classification. *Applied Sciences*, 9(9):1939, 2019.